Full Length Article

The design strategy and testing of an efficient microgas turbine combustor for biogas fuel

Q1

The corrections made in this section will be reviewed and approved by a journal production editor.

Q2

Bahamin Bazooyar bazooyar.bb@gmail.com, ~~Hamidreza Gohari~~Hamidreza ~~Darabkhani~~Gohari Darabkhani~~*~~*

h.g.darabkhani@staffs.ac.uk

~~School of Engineering and Creative Art, Staffordshire University, Stoke-on-Trent ST4 2DE, United Kingdom~~Department of Engineering, Staffordshire University, Stoke-on-Trent, ST4 2DE, United Kingdom

~~*Corresponding author.~~

*Corresponding Author, Professor of Low Carbon and Renewable Energy Systems

Abstract

Nowadays, the design and application of free-carbon emission renewable fuels in micropower generators seem to be interesting to provide decentralized clean, affordable, and resilient energy in developing countries, thereby reaching the 2050 net-zero carbon emission objectives. The operation of micro-scale Closed Cycle Gas Turbine (CCGT) system with these fuels such as biogas without negatively impacting the combustion and micro-turbine performance, should be managed and controlled in the successful design of a micro gas turbine combustor. The application of biogas as a potential fuel due to its low calorific value and impurities, should be made possible in an efficient micro gas turbine combustor design for maintaining NOx emissions, the combustor's ability to light and to tolerate sudden changes in engine load, efficient combustion throughout the engine cycle, and the achievement of the required life. In this work, the efficient design techniques and operation of the 12 [kW] biogas micro-turbine combustor are analyzed and investigated. The designed combustor was manufactured, tested and modeled. Afterward, the emission potential of the designed combustor is discussed and how properly a design scenario for a new fuel should be responded.

Keywords: Combustor design; Microturbine; Biogas; Combustion CFD

1 Introduction

Climate change, global warming and other detrimental impacts of combustion pollutants have mandated strong legislations and regulations in the future design of combustion systems and the choice of fuels [1–7]. The UK targets the 2050 net carbon zero-emission, thereby necessitating the decarbonization of both mobile and stationary combustion systems. Decarbonizing the heat networks usually delivers a major challenge to the designers because the alternatives for conventional hydrocarbon fuels are usually unreliable, intermittent, and impotent to produce the required power.

The boilers and gas turbines usually operate with gaseous fuels to produce heat and power [8]. Both clean alternative fuels and state-of-the-art combustion clean technologies should be utilized to promise a clean environment [9]. Biogas has demonstrated great potentials as a renewable sustainable source of energy for power generation [10]. Biogas can be produced from the decomposition of a variety of flora and fauna waste materials that would otherwise pollute landfills; release toxic chemicals in sewage treatment plants, and waste money, energy, and material [11]. Interest in biogas as a potential fuel has been recently turned out to be increasing for decentralized heat and power generation as there is a

great potential in Subsaharan Africa for biogas production with overly 600 million people without access to any electricity grids. The application of biogas in organic Rankine cycle (ORC) with high capacities turbine combustor was previously revealed possible from both economic [12] and practical point of view [13]. Biogas showed great net present value (NPV) as a sustainable affordable fuel in a wide range of power demands in turbines [14]. However, the application of biogas in small scale turbine power generators may lead to the worst techno-economic conditions [15]. Hosseini et al [16] reported that the high energy and exergy efficiency is achievable in 1.4 [Mw] turbine power with biogas fuel. Nikpey Somehsaraei et al [17] revealed that microturbine mass flow and pressure ratio decreased with biogas fuel and as a result, the surge margin of the turbine will decrease accordingly. Under low powers and temperatures, the use of biogas is more likely to cause surge. Biogas, carbon dioxide could also influence the burning velocity of the biogas flame, possibly leading to the flame blow-off and flame detachment from the fuel nozzle [18]. However, it may increase the radiation and heat transfer of the combustor and flue gas [19]. The biogas fuel can be stabilized using strong swirling flows. Via strong swirling an effective internal recirculation zone will be established and the ignition of the unburned biogas proceeds, thereby stabilizing the biogas fuel with even relatively low burning velocity [20–23]. A strong recirculation zone could also bring about a high fluid residence time, promising effective combustion of the fuel [24]. Dai et al. [25], Lee and Hwang [26] investigated the stability limits of biogas premixed flame and reported that the presence of CO_2 makes it very difficult for biogas flame to be stabilized within a wide range of air and fuel flow rate. The presence of carbon dioxide and other impurities leads to combustion instabilities. Lafay et al [27] observed the biogas flame reactive zone in the central recirculation zone of the microturbine combustor and 16 [Hz] pressure fluctuation frequency with biogas. Another challenge that should be addressed in the design of the low power combustor for biogas fuel is the management and regulation of NO_X emission. Other limitations of biogas fuel that could possibly lead to inferior biogas heat recovery potential, i.e., low wobble index. Liu et al. [28] stated that every microturbine combustor can host fuels with a specific range of Wobble Index (WI) and any deviation may lead to a significant gap between ignition/lean extinction, and either the high NO_X or CO_2 emission. These limitations under low power demands could be successfully managed and overcome with a state-of-the-art design of microcombustor for low power generation applications.

In this study, the design strategy of the 12 [kW] microturbine combustor will be delivered to be used in the Bladon Micro Turbine (MT) Ltd available plenum for biogas fuel which was operating with diesel and kerosene fuel. The designed combustor in terms of performance, optimization, and eco-exo-energy was analyzed in our previous study [29]. Many facts in the design strategy which still remains unknown including techniques to stabilize the biogas flame in small dimensions, flashback avoidance, flame boundaries control, start-up, combustor emission sensitivity to the biogas characteristics will be evaluated. The combustion behavior of the newly designed combustor will be analyzed using various laboratory techniques and numerical analysis. The turbulent biogas flame in the designed combustor was also numerically simulated to extend the understanding of the experimental results. To manage the biogas in the combustor and limits the NO_X emission within a desired range, a viable approach is to make a partially mixed air and biogas within the lean blow-off limit for the beginning of the ignition using air-staging techniques [30]. To have a low NO_X combustor, the premixing of fuel and air will be managed and bounded by the onset and threshold of the combustion stability. This is crucial in the combustor design and will be analyzed in the current study to have a single-digit NO_X combustor.

2 Experimental apparatus and procedures

The combustor is designed by Staffordshire team members, manufactured and tested at the Bladon MicroTurbine Ltd at proving factory, Coventry, United Kingdom. It is equipped with a radial swirler (swirl number = 0.6) that conducts the air into the premixed sleeve to mix with fuel and make a partially premixed before it enters the liner: the main flame holder where it meets fresh hot air at three stages. This part of the design was very sensitive as the partially premixed mixture should be as lean as possible in fuel for controlling the NO_X while it should be below the threshold of blow-off limit so that the ignition begins by mixing with the staging air further downstream. The combustion completes with the injection of air through primary and secondary holes at two stages to avoid the stoichiometric combustion and was diluted with dilution holes to further control and reburn of NO_X. The outer body of the liner was considered corrugated for effective heat transfer and cooling of the internal part of the flame holder and perforated with four series of holes (one series for primary air, one for secondary air and two for dilutions) for the staging of the air. A series of holes in the micro combustor head was also considered to cool down the internal walls and head of the liner. All the dimensions were obtained from the Lefevre method [31] of combustor design for maximum allowable 3% pressure drop overall

and were optimized using validated numerical simulations. In the case of biogas, the shape, orientation, and location of both swirler and injector relative to the combustor main body were important to manage the combustion between the threshold of flashback and blow-off. After the initial parameters were obtained, the combustor was manufactured by the Bladon team and was tested in terms of efficiency, emissions, and other physical characteristics. The data obtained was used for validation of the numerical simulations which from this point forward was used for the optimization of the combustor. The different parts of the micro combustor including photo and geometrical features are shown in Fig. 1.

Fig. 1

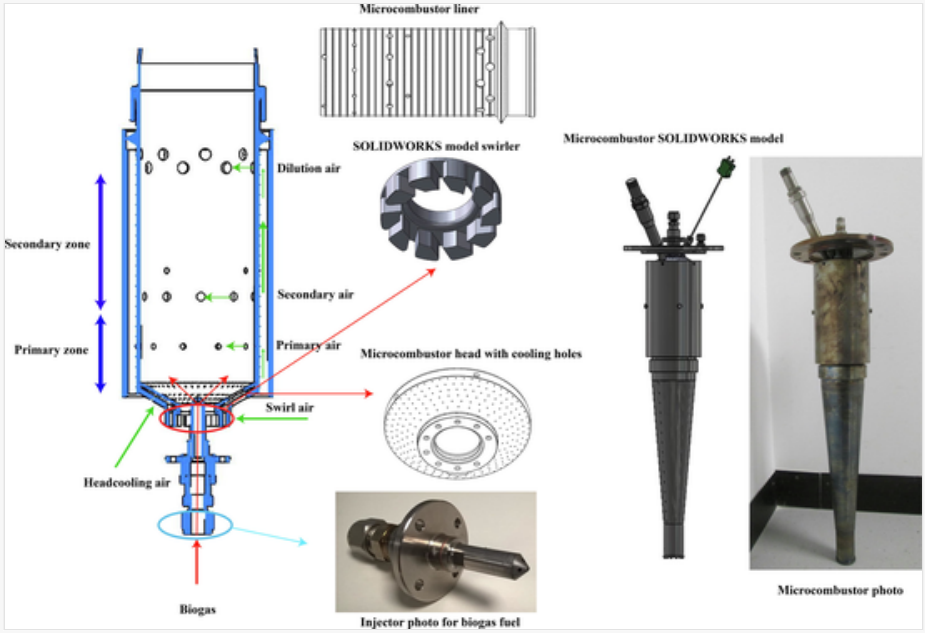

The schematic of the microcombustor for biogas fuel.

The manufactured combustor traverse data and dimensions including length, diameter, and areas of different openings were measured by National Centre in Combustion & Aerothermal Technology, Loughborough University. Loughborough used CO_2 injection to estimate how much dilution air recirculates and concluded that the amount is substantial. The combustor is to be placed in the Bladon MT 12 [kW] microturbine plenum where it is fed with warm air for combustion. To evaluate the operation of the combustor under real MT condition, an experimental rig is utilized with flexible boundary conditions and the ability to take a suitable gas analysis sample. A DEWEsoft data acquisition system was used to record the measurements and to control the operating points of the micro combustor including airflow, fuel-gas flow, and composition. The system reads at 100 [Hz]. Data was reduced by averaging to 1 [Hz] for initial analysis. The data obtained during this time was refined, averaged and reported. The uncertainty for NO_X was around 8% and for CO 5% and temperature and CO_2 below 1%. These variations in the measurement are completely reasonable as the fluid and airflow rates were fluctuating and not constant.

The service to complete emissions measurements was provided by the University of Sheffield Low Carbon Combustion Centre using their Mobile Emissions Laboratory (MEL) with a Model 4000VM Heated Vacuum Chemiluminescent Gas Analyzer. The MEL is equipped to monitor smoke, carbon dioxide, carbon monoxide, nitrogen oxides (NOx), particulates, and unburned hydrocarbons (UHC) with recognized standards. The emissions are sampled through a heated line to enable accurate control of sample temperatures.

A fuel injector system including two mass flow control (MFC) for CH_4 and CO_2 was utilized to control the rate of fuel and CO_2/CH_4 ratio in biogas. The CH_4 and CO_2 were blended in the mixing skid and their proper mixing was promised using a backpressure valve. The Baldon MT combustor test rig (see Bazooyar and Darabkhani [29]) is engineered to control the mass flow, temperature, and pressure inside the micro combustor. The airflow is set via the intel mass flow controller. For realistic tests under the MT conditions, the micro combustor is placed into a heat-exchanger type plenum (i.e., recuperator) which has two sides: a low and high pressure (HP). The combustor inlet temperature is controlled by the temperature and flow through the recuperator low pressure (LP) side. The air is heated and pressurized and then is fed to the high-pressure side of the recuperator. The low-pressure side of the recuperator is fed with high-temperature air from the low pressure vitiated air heater. Heat is transferred to the HP air raising its

temperature to the desired combustor inlet temperature. The combusted mixture is then discharged into a T piece and through an orifice plate. Additional air is added at the T piece, increasing the pressure drop across the orifice and thus controlling the combustor pressure. Finally, more cold air, supplied by two electric blowers is added to reduce the temperature prior to entering the flue.

Fig. 2 gives a photo of the test rig including micro combustor tester, traverse data analysis test cell fuel mixing skid and FTIR gas analyzer. More specification for the entire test rig is given in Table 1.

Fig. 2

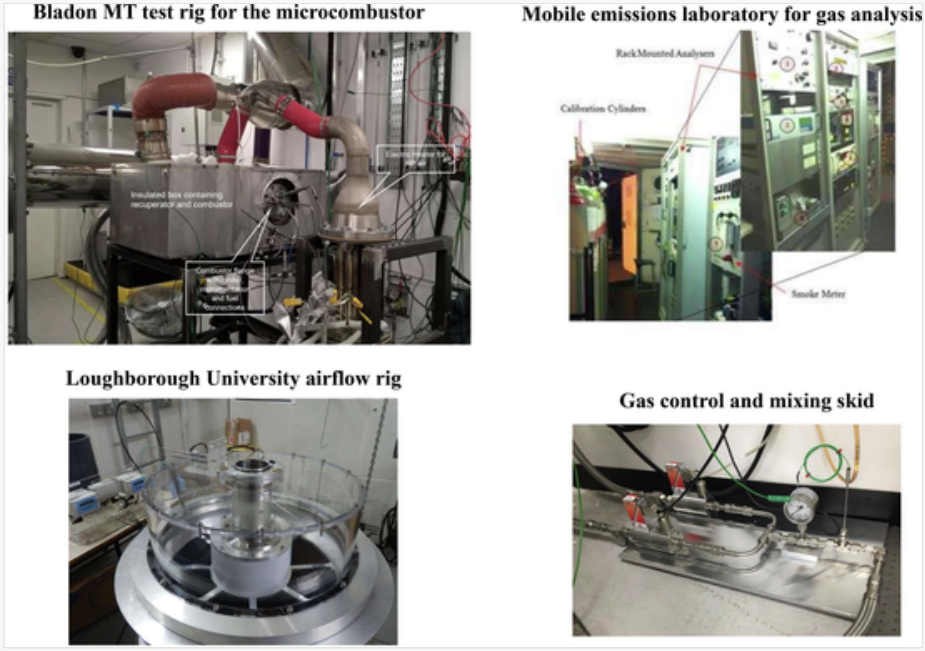

Experimental apparatus: the microcombustor test rig, mobile emissions laboratory for gas analysis, Loughborough University airflow rig, gas control and mixing skid.

Table 1

The table layout displayed in this section is not how it will appear in the final version. The representation below is solely purposed for providing corrections to the table. To preview the actual presentation of the table, please view the Proof.

The specification of the test rig and measurement devices.

Test rig	Specification
Gas control and mixing skid	CH_4 and CO_2 capsule, two MFCs, pressure gauge
Bladon MT facility	Air storage tank, two air blowers, air flow meter, two heaters, air compressors, recuperator, thermocouples, backpressure valve
Loughborough University airflow rig	Perspex plenum chamber, a 5-hole pitot probe
Sheffield 4000VM Heated Vacuum	CO_2, CO, NO + NO_2, UHC, PM, hot pipes

Chemiluminescent Gas Analyzer	

The combustion test was covering a range, representative of the normal running conditions for the MT and fluctuations in the composition of biogas. The schedule, listed different operating points, was developed for efficient movement from one condition to the next. Once tests are stable, a data logging indicator was set to allow post-test extraction and averaging of data from the data recorded within a minute. For the analysis of the results, equivalence ratio (ϕ) is used to show the amount of fuel added rather than Air to Fuel Ratio (AFR). Other determining parameters presented are emission indices, and the combustor exit temperature which is a function of combustor inlet temperature and ϕ with richer mixtures giving a greater temperature rise.

3 Simulation

The Reynolds-Average-Navier-Stokes (RANS) k-ω shear stress transport (SST) [32] is joined with steady diffusion Flamelet [33,34] and discrete ordinates radiation model [40] to give an in-depth insight into the design methodology and effect of different operating points in the 3D computational domain including 30 M grids (Fig. 3.). The combustor solid parts including head, liner, casing swirler, and discharge nozzle were also included in the computational domain for having an accurate estimation about the combustor wall temperature that should promise the lifetime of the combustor using biogas fuel. The outer walls of the combustor were non-slip and adiabatic (as walls were completely isolated), and the outlet was specified by the continuity boundary condition. The mass flow intel was considered for fuel and air (swirl air = 8%, head cooling = 5%, primary air = 8%, secondary = 18% and dilution = 61%), and pressure outlet for the combustor outlet plane. The GRI mesh III [35] reaction mechanism was used to represent the combustion efficiency. Analysis of the flame chemistry will be achieved using the ANSYS Chemkin-PRO using GRI mesh III. The reaction rate terms were modeled using a closed partially stirred reactor (PaSR) model [36], which accounts for the turbulent-chemistry interaction. For NO_X emission, the thermal, prompt NO, and N_2O pathway mechanism models were used to account for the formation of nitrogen oxides in the combustor [37,38]. The NO_X was modeled as the Flamelet concept is not able to show slow chemistry reactions [39]. The extended thermal pathway, De Soete formulation for prompt NO and N_2O pathway were utilized in the current study.

Fig. 3

The computational domain for the analysis of the combustor.

4 Result and discussion

The results of the experimentation and numerical simulation are presented here. The operation of the micro combustor at 35 different operating points were tested and analyzed. Within these 35 operating points was successful and 4 weak/extinction was observed. The influence of the different factors on the design including recuperated air temperature, combustion pressure, equivalence ratio, and carbon dioxide in the biogas on the operation of the micro combustor is verified in terms of emission indices and combustion efficiency. Other design essential variables including pressure drop and lighting are also reported.

The relatively low burning velocity of the biogas could curtail the proper stabilization of the flame in the micro combustor since the longer biogas threshold of ignition requires more resident time of the fuel in the combustor (the same could also happen with fast burning fuels, i.e., hydrogen [41]). This was handled via the design of the proper fuel injector which can inject the biogas fuel with a required low velocity and appropriate location for primary holes to recirculate the combusted materials with a required degree of intensity to counteract the negative influence that a low-velocity nozzle can have on the turbulent mixing. Intense turbulent mixing of the fuel improves the combustion efficiency of the ammonia with the same limitation [42,43].

4.1 Lean blow-off and lit

The mixing and ratio of fuel/air should be well below the blow-off limit, so the mixture is lighted. The flame is not sustained if the velocity of the air surpasses the flame propagation speed. The presence of CO_2 in biogas could shift the blow-off limit of the partially premixed mixture of biogas and air. The experimentation demonstrates that the CO_2 significantly impaired the ignition. CO_2 could either absorbs the combustion heat or dissociate to CO. Therefore, it could deteriorate the combustion and to some extent reduce the NO_X.

Ignition is a complex stochastic phenomenon. The interaction of the fuel and air, turbulence mixing, and temperature should be high enough for igniting the partially premixed mixture of fuel and air that otherwise leads to significant pollutant formation and in worst cases flame extinction. For this combustor, ignition testing was carried out at atmospheric conditions i.e. room temperature and pressure. Ignition is easily determined by the change in rig noise and increase in combustor outlet temperature. For this test, the air and fuel (CH_4 + CO_2) were initially set. After 5 sec when the stream of fuel and air was stabilized, and the required recirculation zone was established in the combustor, the ignitor was turned on. If the ignition is initiated and withstood 10 s, this is a pass lit. 3 consecutive lights are a successful point. When light-up occurs, the fuel flow rate was slowly reduced to find W/E times.

Ignition and extinction are depicted in Fig. 4. Weak extinction is a little more consistent than the light-up and ignition. The designed combustor was lit at 40 [g/s] airflow with pure methane. With 60% methane, it would light above 20 [g/s]. The Loughborough analysis revealed that the designed swirler takes and passes around 14% of recuperated air. If the swirler area was manipulated to pass 7% of the recuperated air, the combustor was lit over a wider range of air flows from 40 to 70 [g/s] at the expense of more NO_X formation. For biogas fuel, the increase in the airflow rate will diminish the gap that existed between the ignition and extinction limits in the same way as natural gas [44]. This was also confirmed by Liu et al. [28]. Despite the deterioration of the biogas ignition and flame stability region associated with the presence of CO_2, our experimentation and those of [45] have confirmed that appropriate use of a swirl combustor can stabilize the biogas flame over a wide range of equivalence ratios. The air swirl intensity of the designed combustor was high enough to stabilize the biogas flame, promising ignition and sustainable combustion.

Fig. 4

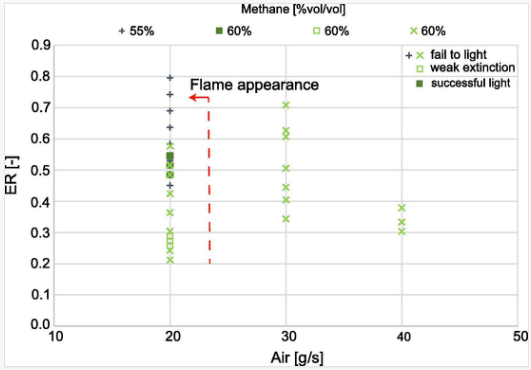

Ignition, extinction, and weak extinction analysis.

4.2 Outlet emissions

The Mobile Emissions Laboratory (MEL) brought on-site by the University of Sheffield Low Carbon Combustion Centre can measure and monitor smoke, carbon dioxide (CO_2), carbon monoxide (CO), nitrogen oxides (NO_X), particulates, and unburned hydrocarbons (UHC) with recognized standards. The emissions are sampled through a heated line to enable accurate control of sample temperatures. A gas sample is taken from the rig downstream of the

combustor and is cooled to around 200 [°C] in a section of pipe chilled by compressed air before being supplied by a heated line to the emissions van.

The in-efficiency, CO, UHC, and NO_X of the combustor are demonstrated in Fig. 5. The emission indices (EI) are reported based on grams of emission per kg of fuel consumed excluding CO_2. The combustor inefficiency is defined $(1-\eta)\%$ with η denoting the combustion efficiency of the combustor. The results are obtained for three different volumetric percentages of methane (60, 50 and 40%) in CO_2 by 31 different operating points. Every operating point is labeled with an indicator for which the initial equivalence ratio and initial combustion air temperature are also reported. The combustion efficiency goes up for the combustor outlet temperature above 1050 [K]. The efficiency is improved by increasing the temperature and methane in the fuel. Between 1000 and 1050 [K], the combustion of biogas with 50% methane is rather inefficient leading to 2.29% and 1.33% in-efficiency in tests 21 and 33. This in-efficiency of the combustor results in poor combustion and significant CO and hydrocarbon pollutants. The CO could form as a result of the poor mixing, incomplete combustion and flame quenching at cold surfaces [39]. The CO for the designed combustor is well below 10 [PPMV] at temperatures above 1100 [K]. The incomplete and poor flame in the combustor emanates intermediate combustion species such as formaldehyde and alkenes forming and knowing as unburned hydrocarbons (UHC) [46–48]. The overall trend of UHC is also similar to those of CO emission and in-efficiency. Above 1050 [K], UHC reaches almost zero for all operating points with whatever the methane content of the fuel. The index of nitrogen oxides ($NO + NO_2$) is also reported at the combustor outlet. For biogas (CH_4 and CO_2), the formation of NO is only via thermal and prompt mechanisms. NO_2 is also kinetically limited to low-temperature combustion [49]. The emission index of NO_X is linearly correlated with outlet temperature. More NO_X will form per kg of fuel burning in the combustor. The presence of CO_2 in the biogas could decrease the NO_X for the same outlet temperature expected from the combustor. At 1150 [K], the emission indices of NO_X are approximately 5.8, 2, and 1.2 for percentages 100, 60 and 50 of methane in biogas, respectively (NOx and CO for flameless biogas combustion 3 ppm and 16 [ppm] [19], for biogas-CH_4::59 [%], CO_2::41@ 100 load, NO_X = 7 [ppmv], CO ≈ 1 [ppmv] [28]).

Fig. 5

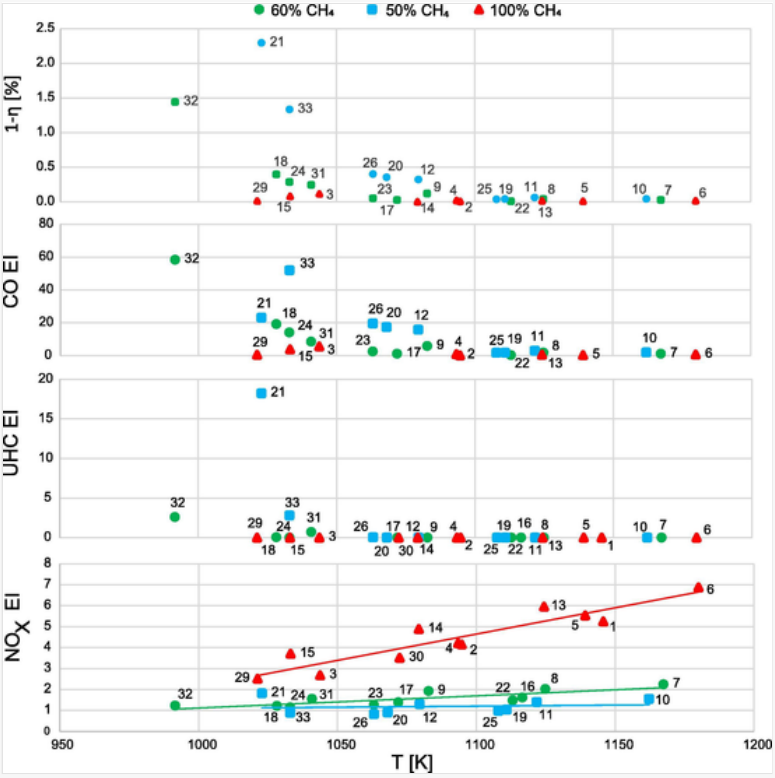

Inefficiency (1-η), CO, UHC, and NO_X analysis.

4.3 CO_2 content

The composition of biogas could be also different depending on the charges timing of the biodigester [11]. The ability of the combustor to operate with a larger proportion of CO_2 in the biogas fuel obviates the need for several numbers of biodigester and costs associated. The combustor rig was therefore tested at higher levels of CO_2 than initially planned,

starting at 32% CH_4. It appears further additional CO_2 only has a small effect on increasing CO with the same kick-up below combustor outlet temperature 1050 K. Therefore, running the combustor at higher CO_2 levels is completely adjusted. NOx continues to fall with increasing CO_2. With the additional CO_2 levels, it is possible to determine a relationship between CO_2 proportion in the fuel and NOx reduction from a baseline at 100% methane. Liu et al. [28] have obtained a same trend between the level of CO_2 in biogas and emissions (CO, NO_X and CO_2).

4.4 Model validation

To analyze the combustor further using CFD results, the verified CFD model was validated using experiments. Table 2 lists the operating points used to validate the model. The results of validation including the model and experimental temperature, CO_2 [%] and NO_X [ppmv] corrected for 15% oxygen content of the flue gas were reported in Fig. 6. The root mean square errors (RMSEs) of the model in relation to the experimentation were 17 [K], 4.99 [ppmv], and 0.38 [%] for temperature, NO_X and CO_2, respectively.

Table 2

Operating points used in experimentation and CFD validation (sorted based on percentage of methane and inlet air temperature).

Test point	Temperature [K]	Pressure [kPa]	CH_4 [%]	CH_4 [g/s]	Air/Fuel
5	893	260.79	100%	0.89	160.9
4	891	259.50	100%	2.55	201.1
6	891	260.51	100%	3.38	134.1
1	854	230.57	100%	0.79	137.0
2	853	232.30	100%	0.74	168.6
3	852	230.18	100%	0.89	219.2
13	831	262.58	100%	2.81	134.1
14	830	261.40	100%	2.13	160.9
15	830	259.93	100%	3.00	201.1
30	776	229.61	100%	2.55	137.0
29	775	227.90	100%	3.38	168.7
7	890	261.48	60%	0.59	134.2
9	889	258.91	60%	2.27	201.3
8	888	260.22	60%	0.74	160.7
22	832	228.83	60%	1.70	136.9
16	832	262.22	60%	2.13	134.2
18	831	260.16	60%	2.25	201.4
24	830	231.43	60%	0.64	199.29
23	829	230.99	60%	2.44	169.0
17	829	259.64	60%	2.81	160.7
32	752	248.90	60%	1.84	169.0
31	748	259.67	60%	0.79	136.96
10	889	261.51	50%	2.27	134.04

11	889	259.77	50%	3.00	161.23
12	889	259.84	50%	0.49	201.37
21	833	262.19	50%	1.56	201.39
26	833	229.47	50%	0.59	168.66
25	831	230.16	50%	1.70	137.19
20	830	261.81	50%	2.25	161.27
19	830	261.08	50%	0.64	134.05
33	748	277.64	50%	1.84	137.18

Fig. 6

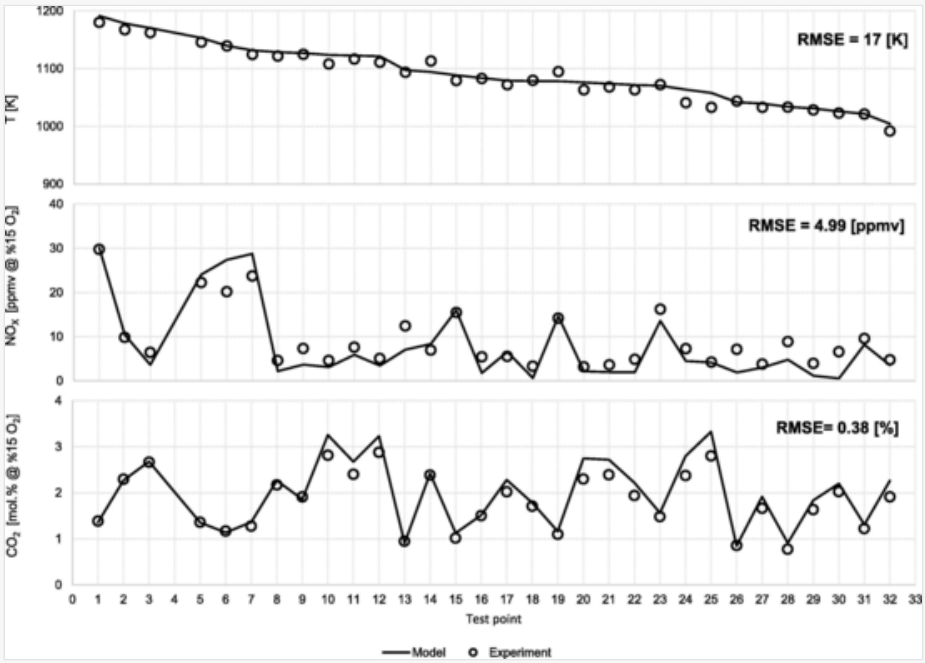

The validation of the CFD modeling results in terms of temperature, CO_2 and NO_X at combustor outlet plane.

The flame structure and stabilization normally depend on the local flow conditions, mixing and design of the combustor [50,51]. Below, the designed combustor will be analyzed in terms of flame stabilization and potential of pollutant formation.

4.5 Flame stabilization

In this combustor, the flame stabilization is achieved via the proper design of the radial swirler and the formation of recirculation zone inside the flame holder. Fig. 7 gives the 3-dimensional streamlines in the primary zone of the combustor and 2 dimensional streamlines at two perpendiculars planes ZX and ZY. Two main recirculation zones have been established at the primary zone that stabilize the flame in the microcombustor and promise a sustianable combustion. The swirler is giving a centrifugal force to the air jet by both rotating the air stream and change of its radial to axial velocity. The secondary recirculation zone appears in the center of the flame holder in the fuel jet stream. The primary and seondary recirculation zones are effectively exchanging materials and their interaction leads to the flame stabilization.

Fig. 7

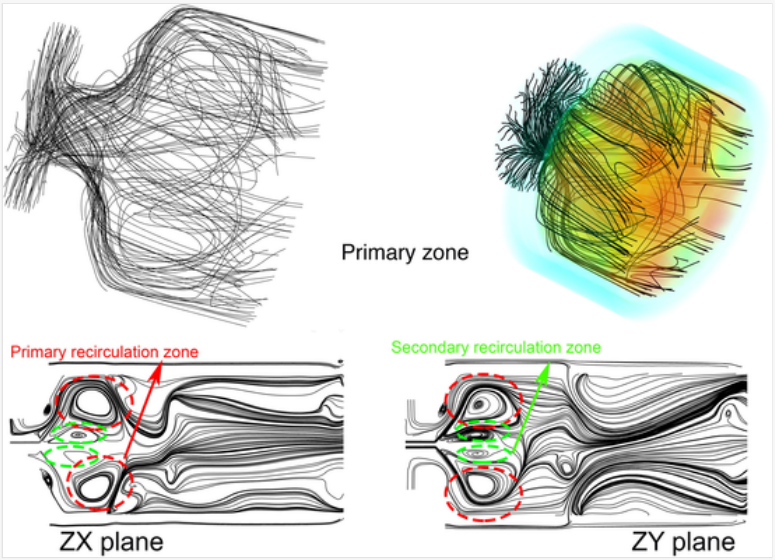

The 3D streamlines in the primary zone along with 2D streamlines at surfaces ZX & ZY of the designed microgas combustion.

4.6 NO_X and CO formation

The biogas fume in the designed combustor is analyzed using iso-surfaces of NO_X and CO in the combustor at the operating point desired to energize the turbine engine. Fig. 8 gives the iso-surfaces of constant CO mole fractions 0.02, 0.005, and 1e-6 on a dry basis for 15% oxygen. It shows the evolution of this deleterious pollutant in the designed combustor. The upper limit for the corrected 15% dry CO was 0.03 (mol fraction). The iso-surfaces for three 0.02, 0.005, and 1e-6 mol fractions are given. The level of CO is significantly going down in the combustion mixture by receiving the air from secondary holes. The volumetric averaged mole fraction of CO between secondary and dilution holes is around 1 [ppm]. After the dilution holes, the level goes down further so as it reaches 0.2 [ppm] in the discharge nozzle at the studied operating point. Fig. 9 gives the evolution of the NO_X with four different iso-surfaces 100, 50, 20, and 14 [ppm] (dried corrected for 15% oxygen). The maximum mole fraction of nitrogen oxides is 0.00016. The effective strategy of air staging controls the level of NO_X in the combusting mixture as it moves forward. The dilution holes bring the level of NO_X down further to 14 ppm at the combustor outlet.

Fig. 8

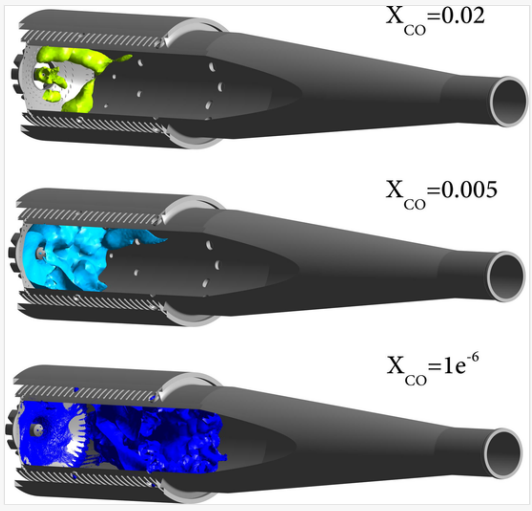

The evolution of CO via constant mol fraction iso-surfaces 0.02, 0.005, and 1e-6 corrected based on 15% excess oxygen.

Fig. 9

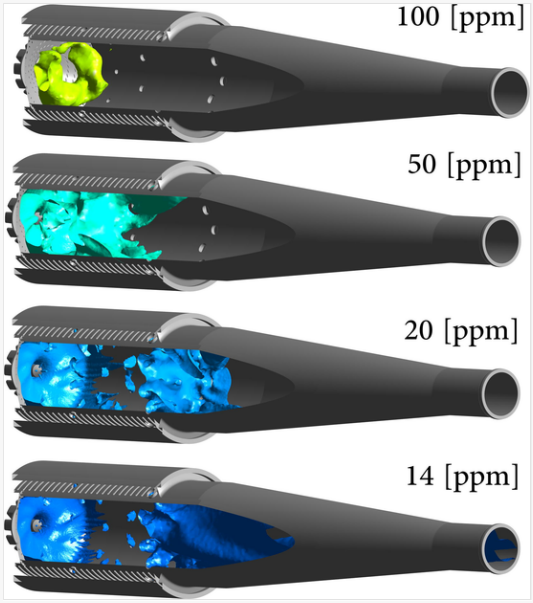

The evolution of NO_X via constant molar concentration iso-surfaces 100, 50, 20 and 14 ppm (corrected based on 15% excess oxygen).

The numerical study confirms that the main combustor pollutants (CO and NO_X) form at the primary zone of the combustor (the volume of the combustor that is before the primary holes). The results reveal that the designed microcombustor was able to control both CO and NO_X emissions by completing the combustion downstream and avoiding stochiometric mixing. The primary zone of the microcombustor is a fuel-rich zone area that has a high potential for CO emission. The mixture in this area will receive air from primary ports and completes the combustion. Fig. 10 gives the axial trend of CO and NO_X emissions, showing the effective air stagging of the combustor in controlling the NO_X emission and destruction of CO emission. The presence of CO_2 in biogas can change the location of the reaction zone and reactions associated with the ignition and NO_X [27]. To further verify the potential of biogas and the design in emitting the pollutants in the primary zone of the combustor, the NO and CO emission pathways were investigated using a closed partially stirred reactor (PaSR). The sensitivity analysis for the presence of CO_2 was obtained for the normalized reaction associated with the NO_X and CO formation. The analysis has shown that the mixture of biogas and swirl air could ignite at temperatures above 1400 K highlighting the role of recirculation zone establishment in sustainable combustion. The analysis of the streamlines (not shown here [29]) at the designed combustor revealed that three recirculation zones have appeared: first near the combustor conic head which is very weak, second near the combustor center between the axial and angled fuel stream and third a little far from the center near the walls extending from the combustor head toward the primary ports. In fact, the central recirculation zone is weaker in intensity providing a partially premised mixture of fuel and air. The third zone is more intense recirculating a part of combusted material toward the mixture biogas/air, thereby promising sustainable combustion. The turbulence-chemistry interaction analysis has shown that the spatial concentration of the combusting mixture in the designed combustor has reached that of the primary port surface after around 0.0063 s. The role of each elementary reaction in the production and destruction of NO is given in Fig. 11 in a primary part of the combustor. Around 40 elementary reactions including thermal, prompt, N_2O pathway mechanisms contribute to the production of nitrogen oxides in biogas fuel. Fig. 11 illustrates the contribution of these reactions into NO_X which has considerable rate of reactions for both pure methane and biogas fuel (57% methane and 43% CO_2) normalized by the nitrogen dissociation reaction ($N_2 + O = NO + N$).

Fig. 10

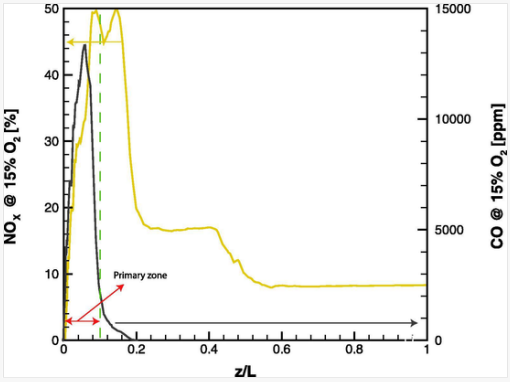

Axial concentrations of CO [ppm] and NO_X [ppm] corrected based on 15% excess air.

Fig. 11

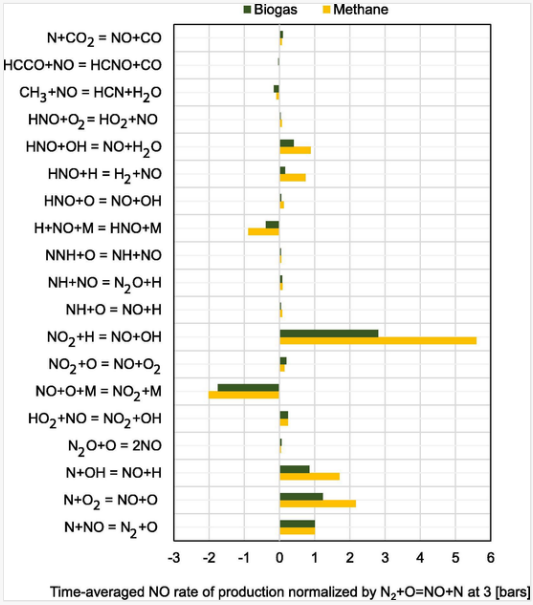

The contribution of elementary reactions in NO emission in the primary zone of the combustor (equivalence ratio, ϕ = 1.02) for methane and biogas/air flame at pressure 3 [bars].

The extended thermal mechanism ($N_2 + O{=}NO + N$, $N + O_2{=}NO + O$, $N + OH{=}NO + H$) along with elementary reaction ($NO_2 + H{=}NO + OH$) are playing the main role in the NO formation of both methane and biogas in the primary regions. The role of CO_2 as methane accompanying gas in biogas fuel in decreasing the NO emission is confirmed in Fig. 11. The prompt NO ($CN + O{=}NO + C$, etc) is also under control despite the richness of this region from the fuel. The presence of CO_2 as a third body in biogas fuel might be anticipated to increase the NO. CO_2 could increase the rate of NO formation through reactions $N_2O + O{=}2NO$, $NO_2 + O{=}NO + O_2$, and $N + CO_2{=}NO + CO$. Carbon dioxide in biogas can also foster the contribution of $CH_3 + NO{=}HCN + H_2O$ and $HCCO + NO{=}HCNO + CO$ in NO destruction in the fuel-rich zone. However, CO_2 influence in increasing of NO is not as much as in decreasing of it. Indeed, carbon dioxide acts as a carrier of the combustion heat, thereby limiting the dissociation of nitrogen and NO thermal mechanism.

The role of CO_2 in incomplete combustion of the biogas fuel in the primary region of the combustor is also investigated by reaction path analysis of the CO emission for both methane and biogas fuel normalized by reaction ($C_2H_2 + O{=}CO + CH_2$). Fig. 12 reveals that the formation of CO is mainly by $O + C_2H_2{=}CO + CH_2$, $HCO + O_2{=}HO_2 + CO$, and $O + CH_3{=}H + H_2 + CO$ and its destruction is via $OH + CO{=}H + CO_2$. Fig. 12 confirms that the presence of the CO_2 in the biogas fuel enriches the primary region of the combustor in two ways of increasing the rate of formation and decreasing the rate of CO destruction. Indeed, the presence of extra CO_2 in the chamber shifts the equilibrium of reaction $OH + CO{=}H + CO_2$ towards the reactant, thereby decreasing the chance of CO destruction. Even though

biogas may have a high level of CO emission compared to methane, the design of the combustor including the proper rate of mixing, dimensions, swirl intensity, and proportion of air and fuel is satisfactorily done as further progress of the combustion completely eradicate the CO emissions downstream. This fact was confirmed in both numerical and experimental studies of the designed combustor.

Fig. 12

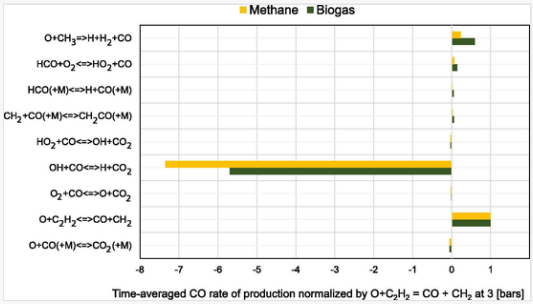

The contribution of elementary reactions in CO emission in the primary zone of the combustor (equivalence ratio, ϕ = 1.02) for methane and biogas/air flame at pressure 3 [bars].

Overall, CO_2 emission in the fuel necessitates considering a trade-off between the combustor ability to light, CO with NO_X in the combustor using biogas. CO_2 in biogas could reduce the NO_X at the expense of combustion deterioration. A good design of the combustor including a proper air staging technique, with the establishment of a strong recirculation zone for enough turbulent mixing, and an appropriate proportion of fuel and air in the primary region brings about a required power with an expected and standardized level of emissions.

5 Conclusion

A new micro combustor for biogas fuel that can be installed in the Bladon MT recuperated air plenum is designed to produce 12 [kW] electrical power. The design technique and strategies for the combustor are proposed and summarized below.

1) To control the level of emission in the biogas combustor, the flame blow-off limit, rate of mixing and proportion of air to fuel in the primary zone of the combustor is essential.

2) The presence of CO_2 in the biogas fuel makes the lighting of the combustor relatively difficult, requiring a very fuel-rich mixture of biogas/air for the start-up of the energy system.

3) CO_2 could help to control the level of nitrogen oxide in the primary zone when the flame front appeared and the potential for NO_X emission was high by accommodating the combustion heat.

4) Even though CO_2 in the biogas could intensify the rate of CO formation and slow down the rate of CO destruction by shifting the equilibrium of the reaction ($OH + CO = H + CO_2$), the successful design of the combustor, its appropriate dimensions, nozzle, etc along with proper control of the flame in the liner from reaching the wall cold surfaces end up with CO emission within an acceptable limit in the primary zone of the combustor and complete destruction of it by the progress of the combustion further downstream.

5) CO_2 as a third body in biogas fuel to some extent increase the rate of NO formation via the N_2O pathway mechanism, although the contribution of this mechanism in NO content in the primary zone is trivial as the pressurized combustion is occurring in the designed combustor. Overall, CO_2 in biogas results in the reduction of NO_X of the biogas compared to methane fuel in the designed combustor.

CRediT authorship contribution statement

Bahamin Bazooyar: Conceptualization, Data curation, Investigation, Methodology, Validation, Visualization, Writing - original draft. **Hamidreza Gohari Darabkhani:** Conceptualization, Formal analysis, Funding acquisition, Investigation, Methodology, Project administration, Resources, Supervision, Writing - review & editing.

Declaration of Competing Interest

The authors declare that they have no known competing financial interests or personal relationships that could have appeared to influence the work reported in this paper.

Acknowledgment

This work is a part of the £1.3 M Micro Turbine Renewable Energy Combustor (MiTREC) project funded ~~project~~ by INNOVATE UK (103502), as part of the Energy Catalyst Round 4 Programme. The authors would like to warmly acknowledge the help and support of Bladon Micro Turbines members (especially Mr Paul Roe and Dr Mike Whiteman), staffs and the management team.

References

The corrections made in this section will be reviewed and approved by a journal production editor. The newly added/removed references and its citations will be reordered and rearranged by the production team.

[1] Noor MM, Wandel AP, Yusaf T. Numerical study of oxygen dilution and temperature distribution of biogas combustion in bluff-body MILD Burner. Proc. 7th Aust. Combust. Symp. (ACS 2013), University of Western Australia; 2013. p. 6–8.

[2] Bazooyar B., Hallajbashi N., Shariati A., Ghorbani A. An investigation of the effect of input air upon combustion performance and emissions of biodiesel and diesel fuel in an experimental boiler. Energy Sources, Part A Recover Util Environ Eff 2014;36(4):383–392.

[3] Noor M.M., Wandel A.P., Yusaf T. Effect of air-fuel ratio on temperature distribution and pollutants for biogas mild combustion. Int J Automot Mech Eng 2014;10:1980–1992.

[4] Bazooyar B., Ghorbani A., Shariati A. Physical properties of methyl esters made from alkali-based transesterification and conventional diesel fuel. Energy Sources, Part A Recover Util Environ Eff 2015;37(5):468–476.

[5] Ghorbani A., Bazooyar B., Shariati A., Jokar S.M., Ajami H., Naderi A. A comparative study of combustion performance and emission of biodiesel blends and diesel in an experimental boiler. Appl Energy 2011;88(12):4725–4732.

[6] Bazooyar B., Shariati A. A comparison of the emission and thermal capacity of methyl ester of corn oil with diesel in an experimental boiler. Energy Sources, Part A Recover Util Environ Eff 2013;35(17):1618–1628.

[7] Bazooyar B., Shaahmadi F., Anbaz M.A., Jomekian A. Intelligent modelling and analysis of biodiesel/alcohol/glycerol liquid-liquid equilibria. J Mol Liq 2021;322:114972. doi:10.1016/j.molliq.2020.114972.

[8] Bazooyar B., Darabkhani H.G. Design procedure and performance analysis of a microturbine combustor working on biogas for power generation. Proc ASME Turbo Expo 2019;4B–2019.

[9] Bazooyar B., Shariati A., Hashemabadi S.H. Economy of a utility boiler power plant fueled with vegetable oil, biodiesel, petrodiesel and their prevalent blends. Sustain Prod Consum 2015;3:1–7.

[10] Hosseini S.E., Wahid M.A. Development of biogas combustion in combined heat and power generation. Renew Sustain Energy Rev 2014;40:868–875.

[11] Vitázek I., Klúčik J., Uhrinová D., Mikulová Z., Mojžiš M. Thermodynamics of combustion gases from biogas. Res Agric Eng 2017;62(Special Issue):S8–S13.

[12]

Sung T., Kim S., Kim K.C. Thermoeconomic analysis of a biogas-fueled micro-gas turbine with a bottoming organic Rankine cycle for a sewage sludge and food waste treatment plant in the Republic of Korea. Appl Therm Eng 2017;127:963–974.

[13] Kim S., Sung T., Kim K. Thermodynamic performance analysis of a biogas-fuelled micro-gas turbine with a bottoming organic rankine cycle for sewage sludge and food waste treatment plants. Energies 2017;10.

[14] Basrawi F., Ibrahim T.K., Habib K., Yamada T., Daing Idris D.M.N. Techno-economic performance of biogas-fueled micro gas turbine cogeneration systems in sewage treatment plants: effect of prime mover generation capacity. Energy 2017;124:238–248.

[15] Basrawi F., Ibrahim H., Yamada T. Optimal unit sizing of biogas-fuelled micro gas turbine cogeneration systems in a sewage treatment plant. Energy Procedia 2015;75:1052–1058.

[16] Hosseini S.E., Barzegaravval H., Wahid M.A., Ganjehkaviri A., Sies M.M. Thermodynamic assessment of integrated biogas-based micro-power generation system. Energy Convers Manag 2016;128:104–119.

[17] Nikpey Somehsaraei H., Mansouri Majoumerd M., Breuhaus P., Assadi M. Performance analysis of a biogas-fueled micro gas turbine using a validated thermodynamic model. Appl Therm Eng 2014;66(1–2):181–190.

[18] Liu H., Wang Y., Yu T., Liu H., Cai W., Weng S. Effect of carbon dioxide content in biogas on turbulent combustion in the combustor of micro gas turbine. Renew Energy 2020;147:1299–1311.

[19] Colorado A.F., Herrera B.A., Amell A.A. Performance of a Flameless combustion furnace using biogas and natural gas. Bioresour Technol 2010;101(7):2443–2449.

[20] Valera-Medina A., Syred N., Griffiths A. Visualisation of isothermal large coherent structures in a swirl burner. Combust Flame 2009;156(9):1723–1734.

[21] Bazooyar B., Darabkhani H.G. Design and numerical analysis of a 3 kWe flameless microturbine combustor for hydrogen fuel. Int J Hydrogen Energy 2019;44(21):11134–11144.

[22] Terasaki T., Hayashi S. The effects of fuel-air mixing on NOx formation in non-premixed swirl burners. Symp Combust 1996;26(2):2733–2739.

[23] Syred N. A review of oscillation mechanisms and the role of the precessing vortex core (PVC) in swirl combustion systems. Prog Energy Combust Sci 2006;32(2):93–161.

[24] Reddy V.M., Katoch A., Roberts W.L., Kumar S. Experimental and numerical analysis for high intensity swirl based ultra-low emission flameless combustor operating with liquid fuels. Proc Combust Inst 2015;35(3):3581–3589.

[25] Dai W., Qin C., Chen Z., Tong C., Liu P. Experimental studies of flame stability limits of biogas flame. Energy Convers. Manag. 2012;63:157–161.

[26] Lee C.-E., Hwang C.-H. An experimental study on the flame stability of LFG and LFG-mixed fuels. Fuel 2007;86(5–6):649–655.

[27] Lafay Y., Taupin B., Martins G., Cabot G., Renou B., Boukhalfa A. Experimental study of biogas combustion using a gas turbine configuration. Exp Fluids 2007;43(2–3):395–410.

[28] Liu A., Yang Y., Chen L., Zeng W., Wang C. Experimental study of biogas combustion and emissions for a micro gas turbine. Fuel 2020;267:117312. doi:10.1016/j.fuel.2020.117312.

[29] Bazooyar B., Gohari Darabkhani H. Design, manufacture and test of a micro-turbine renewable energy combustor. Energy Convers Manag 2020;213:112782. doi:10.1016/j.enconman.2020.112782.

[30]

Bazooyar B., Shariati A., Hashemabadi S.H. Characterization and reduction of NO during the combustion of biodiesel in a semi-industrial boiler. Energy Fuels 2015;29(10):6804–6814.

[31] Ford T. Gas turbine combustion. vol. 62. CRC Press; 1990.

[32] Menter F.R. Two-equation eddy-viscosity turbulence models for engineering applications. AIAA J 1994;32(8):1598–1605.

[33] Peters N. Laminar diffusion flamelet models in non-premixed turbulent combustion. Prog Energy Combust Sci 1984;10(3):319–339.

[34] Peters N. Laminar flamelet concepts in turbulent combustion. Symp Combust 1988;21(1):1231–1250.

[35] Smith GP, Golden DM, Frenklach M, Moriarty NW, Eiteneer B, Goldenberg M, et al. GRI-Mech 3.0. URL Http//Www Me Berkeley Edu/Gri_mech; 2012.

[36] Correa S.M. Turbulence-chemistry interactions in the intermediate regime of premixed combustion. Combust Flame 1993;93(1–2):41–60.

[37] Bazooyar B., Ebrahimzadeh E., Jomekian A., Shariati A. NOx formation of biodiesel in utility power plant boilers. Part a: Influence of fuel characteristics. Energy Fuels 2014;28(6):3778–3792.

[38] Bazooyar B., Hashemabadi S.H., Shariati A. NOX formation of biodiesel in utility power plant boilers; Part B. Comparison of NO between biodiesel and petrodiesel. Fuel 2016;182:323–332.

[39] Bazooyar B., Shariati A., Hashemabadi S.H. Turbulent non-premixed combustion of rapeseed methyl ester in a free shear swirl air flow. Ind Eng Chem Res 2016;55(45):11645–11663.

[40] Selçuk N, Kayakol N. Evaluation of discrete ordinales method for radiative transfer in rectangular furnaces. Int J Heat Mass Transf 1997;40:213–22.

[41] Bazooyar B., Gohari Darabkhani H. Analysis of flame stabilization to a thermo-photovoltaic micro-combustor step in turbulent premixed hydrogen flame. Fuel 2019;257:115989. doi:10.1016/j.fuel.2019.115989.

[42] Pratt DT. Performance of ammonia-fired gas-turbine combustors. CALIFORNIA UNIV BERKELEY THERMAL SYSTEMS DIV; 1967.

[43] Okafor E.C., Somarathne K.D.K.A., Hayakawa A., Kudo T., Kurata O., Iki N., et al. Towards the development of an efficient low-NOx ammonia combustor for a micro gas turbine. Proc Combust Inst 2019;37(4):4597–4606.

[44] Liu K, Martin P, Sanderson V, Hubbard P. Effect of change in fuel compositions and heating value on ignition and performance for siemens SGT-400 DRY low emission combustion system. Proc. ASME Turbo Expo, vol. 1 A; 2013.

[45] Živković M., Milivojević A., Adžić M. Experimental investigation on emission and stability of dual feed biogas swirl combustor. J Renew Sustain Energy 2016;8(2):023104. doi:10.1063/1.4945571.

[46] Bazooyar B., Hosseini S.Y., Moradi Ghoje Begloo S., Shariati A., Hashemabadi S.H., Shaahmadi F. Mixed modified Fe2O3-WO3 as new fuel borne catalyst (FBC) for biodiesel fuel. Energy 2018;149:438–453.

[47] Bazooyar B., Jomekian A., Shariati A. Analysis of the formation and interaction of nitrogen oxides in a rapeseed methyl ester nonpremixed turbulent flame. Energy Fuels 2017;31(8):8708–8721.

[48] Ghorbani A., Bazooyar B. Optimization of the combustion of SOME (soybean oil methyl ester), B5, B10, B20 and petrodiesel in a semi industrial boiler. Energy 2012;44(1):217–227.

[49] Bazooyar B., Ghorbani A., Shariati A. Combustion performance and emissions of petrodiesel and biodiesels based on various vegetable oils in a semi industrial boiler. Fuel 2011;90(10):3078–3092.

[50] Bazooyar B., Jomekian A., Karimi-Sibaki E., Habibi M., Gohari Darabkhani H. The role of heat recirculation and flame stabilization in the formation of NOX in a thermo-photovoltaic micro-combustor step wall. Int J Hydrogen Energy 2019;44(47):26012–26027.

[51] Bazooyar B., Shariati A., Khosravi-Nikou M., Hashemabadi S.H. Numerical analysis of nitrogen oxides in turbulent lifted H2/N2 cabra jet flame issuing into a vitiated coflow. Int J Hydrogen Energy 2019;44(26):13932–13952.

Highlights

- A new 12 kWe microturbine combustor is designed for biogas fuel.
- The experimental analysis of the combustor was carried out at different operating points.
- The combustor was modeled, and the model validated against experimental data.
- The model was used for in depth analysis of the combustor (emissions and reactions).

Queries and Answers

Q1

Query: Your article is registered as a regular item and is being processed for inclusion in a regular issue of the journal. If this is NOT correct and your article belongs to a Special Issue/Collection please contact T.Boopathy@elsevier.com immediately prior to returning your corrections.

Answer: Yes

Q2

Query: The author names have been tagged as given names and surnames (surnames are highlighted in teal color). Please confirm if they have been identified correctly.

Answer: updated